

Short hairpin RNAs targeting Bcl-xL modulate senescence and apoptosis following SN-38 and irinotecan exposure in a colon cancer model

S. M. Guichard · M. L. Hua · P. Kang ·
J. S. Macpherson · D. I. Jodrell

Received: 31 July 2006 / Accepted: 18 December 2006 / Published online: 2 February 2007
© Springer-Verlag 2007

Abstract Bcl-xL is an anti-apoptotic protein over-expressed in colorectal cancers acting on both the intrinsic and extrinsic pathways. We stably expressed four different short hairpin RNA (pSNG-xL1-4) targeting Bcl-xL in HCT 116 cells. HCT 116 pSNG-xL#1 produced a modest (30%) decrease in Bcl-xL expression whilst Bcl-2 levels were similar to the parental cell line, HCT 116 pSNG-xL#2 and 3 showed 50% decrease in Bcl-xL and stable Bcl-2. HCT 116 pSNG-xL#3 showed a concomitant decrease (50%) in Bcl-2. A decrease in Bcl-xL sensitised cells to the small molecule inhibitor of Bcl-xL, Antimycin A3 and the DNA topoisomerase I inhibitors, SN-38 and camptothecin, but not to doxorubicin. HCT 116 pSNG-xL#1 produced a moderate increase in both senescence and apoptosis and a limited increase in SN-38 induced cell death while HCT 116 pSNG-xL#2 produced an increase in apoptosis but reduced senescence. Finally, when both Bcl-xL and Bcl-2 were decreased to a similar degree (HCT 116 pSNG-xL#3), senescence was significantly increased but apoptosis was limited. This effect was confirmed in vivo after administration of irinotecan and was associated with greater anti-tumour effect. Optimal growth inhibitory effect was therefore observed when both Bcl-xL and Bcl-2 were decreased to a similar extent. Antimycin A3, in combination with SN-38 recapitulated this phenotype in HCT 116 cells, suggesting a

potential role for small molecule inhibitors of Bcl-xL/Bcl-2 in the treatment of colorectal cancer, potentially in combination with irinotecan.

Keywords Bcl-xL siRNA · HCT 116 · Senescence · Apoptosis

Introduction

Cellular senescence is a signal transduction program leading to permanent cell cycle arrest. Whilst replicative senescence has long been recognised during aging, a senescence like phenotype (SLP) has more recently been implicated in response to drug treatment in cancer [21]. Indeed, drugs inducing DNA damage and modifying DNA structure such as doxorubicin, etoposide and topoisomerase I inhibitor SN-38 induce terminal growth arrest [4, 11]. SLP is characterised by an absence of telomere shortening, normally observed during replicative senescence [13] and expression of high levels of SA- β galactosidase [4, 27].

The Bcl-2 family includes both pro-apoptotic (Bax, Bak) and anti-apoptotic (Bcl-2, Bcl-xL) proteins, which play a crucial role in mitochondria-driven cell death. Overexpression of the anti-apoptotic protein Bcl-2 has been shown to induce prolonged drug-induced growth arrest and SLP, potentially inducing resistance [20]. Moreover, Bcl-2 was required to maintain c-Myc induced B cell lymphoma in vivo [17]. Bcl-xL over-expression has been shown to reduce the sensitivity to various cytotoxic agents in murine hepatocytes [12], the colon cancer cell line DLD1 [35], and the ovarian cancer cell line, A2780 [33].

S. M. Guichard (✉) · M. L. Hua · P. Kang ·
J. S. Macpherson · D. I. Jodrell
CRUK Pharmacology and Drug Development Group,
Cancer Research UK Centre, University of Edinburgh,
Crewe Road, Edinburgh EH4 2XR, UK
e-mail: Sylvie.guichard@cancer.org.uk

However, Bcl-xL has broader functions than Bcl-2 as it can inhibit TNF-induced cell death by inhibiting DISC formation while Bcl-2 does not [32]. In colorectal cancer, Bcl-xL expression was shown to be higher in carcinomas than in normal mucosa in a high proportion of samples (83%) while Bcl-2 expression was often decreased in carcinomas compared to normal mucosa [2, 18].

Bcl-2 and Bcl-xL are appealing drug targets as they can either be used to decrease cell death after ischemia for example, or increase cell death in cancer [16]. Different approaches have been developed to inhibit these two proteins: antisense oligonucleotides targeting Bcl-2 or Bcl-xL mRNA, and now small molecule antagonists such as antimycin A3 or ABT-737 [23] targeting the proteins. Previous studies from our laboratory have shown that Bcl-xL downregulation using antisense oligonucleotides in the context of wild type p53, increases the cytotoxicity of topoisomerase I inhibitor SN-38, by switching cell death from senescence to apoptosis [11]. However, the phase I study using this antisense (ISIS 15999) confirmed the limited tissue distribution of oligonucleotide antisense and their limited application as systemic therapies [31]. The expression of short hairpin RNA has been shown, at least in vitro, to be more powerful in down-regulating target proteins than antisense oligonucleotides [3]. In addition, short interfering RNA have been investigated in vivo and shown promising results [9]. In this study, we stably transfected HCT 116 colon cancer cells with four different short hairpin RNA targeting Bcl-xL. We validated the HCT 116 pSNG-xL isogenic cell lines generated by determining their sensitivity to Antimycin A3, an inhibitor of Bcl-xL and Bcl-2. We investigated the growth inhibitory effect of topoisomerase I inhibitors SN-38 and camptothecin and topoisomerase II inhibitor doxorubicin against the HCT 116 pSNG-xL cells and evaluated the extent of drug-induced senescence after downregulation of Bcl-xL and/or Bcl-2 both in vitro and in vivo.

Materials and methods

Materials

Camptothecin was purchased from SIGMA. Antimycin A3 was obtained from the National Cancer Institute (Bethesda, MA, USA). Two mM aliquots in dimethylsulfoxide (DMSO) were stored at -80°C . Primers were provided by Cancer Research UK research services (Clare Hall, London, UK).

Cell culture

HCT-116 cells were obtained from the European Collection of Cell Cultures (Salisbury, UK). Cells were grown in monolayer in RPMI 1640 medium supplemented with 5% FCS and 1% L-glutamine at 37°C in a humidified atmosphere containing 5% CO_2 . Stable transfectants were grown in presence of 500 $\mu\text{g}/\text{ml}$ of geneticin[®] (Invitrogen).

Vector constructs

Four 64-mer oligonucleotides targeting Bcl-xL mRNA were designed according to Tuschl's recommendations [28] and inserted in pSUPER-Neo-GFP vector (pSNG) (oligoengine, Seattle, WA, USA). The target sequences are located between 193–211 (#1), 489–507 (#2), 605–623 (#3) and 834–852 (#4) nucleotides in the Bcl-xL mRNA. A shRNA targeting the luciferase gene (pSNG-Luc) according to the sequence published by Elbashir et al. [10] was used as control siRNA. HCT 116 and HT-29 cells were transfected with 2 μg of the different constructs using Effectene[®] reagent (Qiagen, Crawley, UK) and the shRNA-expressing population was selected with geneticin[®] (Invitrogen) at the concentration of 500 $\mu\text{g}/\text{ml}$.

RNA isolation and real-time quantitative RT-PCR

RNA was isolated using Tri-Reagent (Sigma-Aldrich, Irvine, UK). Bcl-xL and Bcl-2 mRNA levels were determined using Quantitect[®] SYBR green RT-PCR kit (Qiagen, Crawley, UK) on Rotorgene 3000 (Corbett Research, Cambridge, UK). Five ng of total RNA were used per reaction. The following primers were used: Bcl-xL F: 5'ttggacaatggactgggtga, Bcl-xL R: 5'ctccgattcagtccctctg, Bcl-2 F: 5'tccatgtcttgacaacca, Bcl-2 R: 5'ctccaccagtgttccatct. 18S was used as reference gene (18S F: 5'aaacggctaccacatccaag and 18S R: 5'cctccaatggatccctcgta). Amplification conditions were as follows: 15 s at 94°C (denaturation), 30 s annealing and 30 s at 72°C (extension) for 45 cycles. The annealing temperatures were 57°C for Bcl-xL, 56°C for Bcl-2 and 55°C for 18S. HCT 116 RNA was serially diluted to build the standard curves. Results are expressed as ratios between Bcl-xL or Bcl-2 and 18S.

Detection of Bcl-xL and Bcl-2 by Immunoblotting

Cells were resuspended in 100 μl million cells of lysis buffer [50 mM HEPES (pH 7.4), 1% Triton X-100, 0.5% sodium deoxycholate, 150 mM sodium chloride,

5 mM EDTA with protease inhibitors pepstatin A 2 µg/ml, aprotinin 10 µg/ml, leupeptin 10 µg/ml, and phenylmethylsulfonyl fluoride 100 µg/ml]. Twenty µg aliquots of total protein were denatured in loading buffer (95°C, 5 min), electrophoresed on a 10% SDS-PAGE gel, and transferred to a polyvinylidene fluoride Immobilon-P transfer membrane (Millipore). Membranes were blocked in 5% fat-free milk powder (Marvel; Premier Brands) in TBS (pH 7.5) with 0.1% TBS-T for 1 h at room temperature, incubated with primary antibody in 5% Marvel in TBS-T 1 h at room temperature and washed in TBS-T, and incubated with secondary antibody conjugated to horse-radish peroxidase (1 h at room temperature). After additional washing in TBS-T and TBS, blots were visualized by chemiluminescence (Santa Cruz Biotechnology).

Cytotoxicity assay *in vitro*

Drug concentrations that inhibited 50% of cell growth (IC_{50}) were determined using the sulforhodamine B technique [24]. Cells were plated on day 1 in 96-well plates at a density of 2,500 cells/well for HCT 116 and the different isogenic cell lines. Cells were treated on day 2 with increasing concentrations of drug for 24 h. After drug exposure, cells were washed once with cold phosphate buffered saline (PBS) and placed in 200 µl of drug-free medium for 72 h after the end of drug exposure. The cells were then fixed with trichloracetic acid and stained with sulforhodamine B. Optical densities were measured at 540 nm with a Biohit BP-800 (Bio-Hit, Helsinki, Finland). Growth inhibition curves were plotted as percentage of control cells and IC_{50} s were determined by Graphpad Prism 3 Software (Graphpad Software, San Diego, CA, USA) using a sigmoidal curve fitting with variable slope. The goodness of fit determined by r^2 was greater than 0.9 and the Hill coefficient <-1 . The results are based on 3–4 independent experiments performed in triplicate and are presented as mean and 95% confidence intervals. For the combination study of SN-38 and AA3, HCT 116 cells were exposed to SN-38 for 24 h followed by AA3 for 24 h. Median effect analysis was used to determine the interactions between SN-38 and AA3. Dose response interactions (antagonism, additivity, synergism) were expressed as a non exclusive case combination index (CI) for every fraction affected or killed (Fa), using the method of Chou and Talalay [7] and CalcuSyn software. A CI <1 indicates synergism, >1 indicates antagonism, and CI value of 1 indicates additivity of the drugs.

Determination of SA β -galactosidase activity

HCT 116 pSNG-xL clones were plated in 24-well plates (10^4 cells/well). Cells were treated with SN-38 0.5, 1, 2.5, 5 and 10 nM, 10^{-9} M for 24 h. Cells were washed with PBS and grown in drug-free medium for 8 days. SA- β gal activity was detected after fixing the cells with freshly prepared 2% formaldehyde solution in PBS. Cells were incubated overnight at 37°C in presence of a staining solution containing 1 mg/ml X-Gal, 5 mM of potassium ferricyanide, 5 mM potassium ferrocyanide 2 mM magnesium chloride in a 40 mM citrate/sodium phosphate solution pH 6. Cells were examined under the microscope and the proportion of enlarged blue cells was estimated from 2,400 cells distributed in 12 different areas within the wells.

Quantification of senescent cell fraction using PKH2 labelling and propidium iodide staining

Drug-induced senescence associated with prolonged cell cycle arrest was determined by PKH2 labelling as described by Chang et al. [4]. Briefly, cells were labelled with the lipophilic fluorophore PKH2 (SIGMA) according to manufacturer's instructions and 10^6 cells were plated in 100 mm Petri dishes. The following day, cells were exposed to 5 nM SN-38 for 24 h. Surviving cells were harvested on day 8, fixed with ethanol, and stained with propidium iodide (20 µg/ml final concentration). The fraction of cells presenting high PKH2 fluorescence (FL1 fluorescence >100) and DNA content $>4N$ (senescent-like phenotype) was calculated in SN-38 treated samples and compared with untreated cells.

Mitochondria membrane potential detection by JC-1 staining

Mitochondrial membrane potential was detected using JC-1 cationic dye (Molecular probes, Cambridge, UK) according to manufacturer's instructions. Briefly, cells were exposed to 100 nM CPT for 24 h. Forty-eight hours after the end of drug exposure, 5×10^5 cells were collected, washed once with ice cold PBS, stained with 0.5 ml 1 × JC-1 reagent and then incubated at 37°C in a 5% CO₂ for 15 min. After incubation, cells were washed twice with 2 ml cell culture medium and re-suspended in 0.5 ml complete medium. Samples were analysed on a Becton-Dickinson FACSCalibur recording both FL 1 (green) and FL 2 (red) fluorescence. Results are expressed as the decrease in FL 2 fluorescence between untreated and treated cells.

Establishment of xenografts in immunodeficient animals

All experiments were conducted according to UK-CCR guidelines and under a project license issued by UK Home Office. Eight-week-old, athymic mice (CS7BP6 *Nu/Nu*; Cancer Research UK), about 20–22 g body weight, were inoculated subcutaneously on both flanks with 10^7 HCT 116 pSNG and HCT 116 pSNG-xL#3 cells in 0.2 ml of serum-free RPMI. The xenograft tumours were measured every 2 days using callipers and tumour volumes were calculated by the following equation: $V = [L \times (W^2/2)]$, where L is length and W is the width].

Efficacy of CPT-11 treatment in HCT 116 pSNG-xL xenografts

After xenografts reached 50–100 mm³, animals were treated with 5 mg/kg irinotecan (pro-drug of SN-38) ip for five consecutive days. Control animals were treated with saline. Tumour response was assessed by the time for each individual xenograft to reach five times their initial volumes and presented as Kaplan–Meier curves. Animals were weighed every 2 days and toxicity was assessed by weight loss.

Detection of apoptosis and senescence in vivo after irinotecan treatment

Xenograft tumours from HCT 116 pSNG and HCT 116 pSNG-xL#3 cell lines were implanted as in the efficacy study. Irinotecan was administered at a dose of 5 mg/kg irinotecan ip. Four tumour xenografts were collected on days 3, 5 and 7 after the start of the treatment and snap-frozen in liquid nitrogen. Cryosections were prepared from each xenograft (three sections/slide) and stored at –70°C until analysis. For senescence, SA- β Gal activity was detected on xenograft cryosections. Cryosections were rapidly warmed at room temperature and fixed with freshly prepared 2% formaldehyde solution in PBS. Slides were mounted on Sequenzae® chambers (Shandon) and incubated overnight at 37°C in staining solution as described for in vitro studies. After the incubation, the staining solution was removed and slides were mounted in Aquatex mounting medium (BDH, Poole, UK). The results are expressed as the total number of senescent cells from three cryosections for each individual tumour.

Apoptosis was detected by TUNEL assay on cryosections. Cryosections were rapidly warmed at room temperature and fixed with freshly prepared 2% formaldehyde solution in PBS. Slides were mounted on

Sequenzae® chambers (Shandon) and apoptotic cells were stained using *in situ* Cell Death Detection kit (Roche, Basel, Switzerland) according to manufacturer's instructions.

Results

The expression of short hairpin RNA targeting Bcl-xL leads to differential downregulation of Bcl-xL and Bcl-2

The expression of both Bcl-xL (Fig. 1a) and Bcl-2 (Fig. 1b) was determined by quantitative RT-PCR in parental HCT 116 and the different isogenic cell lines expressing either a control siRNA (pSNG-Luc) or siRNA targeting Bcl-xL (pSNG-xL#1–4). The expression of a control siRNA targeting the luciferase gene in HCT 116 did not alter the levels of either Bcl-xL (Bcl-xL/18S = 1.0 ± 0.07 and 1.0 ± 0.13 for HCT 116 and HCT 116 pSNG-Luc, respectively) or Bcl-2 mRNA (1.0 ± 0.14 and 0.8 ± 0.12 for HCT 116 and HCT 116 pSNG-Luc, respectively). Three out of four cell lines expressing a shRNA against Bcl-xL showed 30–60% decrease in Bcl-xL expression. HCT 116 pSNG xL#3 also showed a decrease in Bcl-2 expression. HT-29 cells transfected with construct#3 showed an 80% decrease in Bcl-xL expression. However, whilst the parental cell line express very low levels of Bcl-2, both HT-29 pSNG and HT-29 pSNG-xL#3 showed an increase in Bcl-2 expression.

Immunoblot analysis confirmed the downregulation observed at the mRNA levels: HCT 116 pSNG xL#3 showed the lowest expression of both Bcl-xL and Bcl-2 (Fig. 1c).

Downregulation of Bcl-xL sensitises HCT 116 cells to antimycin A3

Antimycin A3 (AA3) binds and inhibits both Bcl-xL and Bcl-2 [29]. In order to validate the specificity of the siRNA expressed, we determined the growth inhibition of AA3 in six colon cancer cell lines and in the different HCT 116 pSNG-xL cell lines (Table 1). The colon cell lines tested displayed very similar IC₅₀ values (from 0.37 μ M in HCT8 to 0.7 μ M in HCT 116), potentially due to the similar levels of Bcl-xL expressed among the cell lines tested (Fig. 1c). However, the growth inhibitory effect of AA3 was greater in the isogenic cell lines expressing a siRNA against Bcl-xL. The gain in sensitivity correlated with the decrease in Bcl-xL expression but HCT 116 pSNG-xL#3, showing a decrease in both Bcl-xL and Bcl-2 was the most sensi-

Fig. 1 Expression of Bcl-xL (Filled box) and Bcl-2 (Open box) in colon cancer cell lines. mRNA expression of Bcl-xL (a) and Bcl-2 (b) in HCT 116 and HT-29 cells expressing short hairpin RNA against Bcl-xL. Results are normalised with 18S rRNA expression and are mean of 2–3 experiments performed in triplicate. c Bcl-xL and Bcl-2 protein expression in six colon cancer cell lines and the different HCT 116 pSNG-xL cell lines

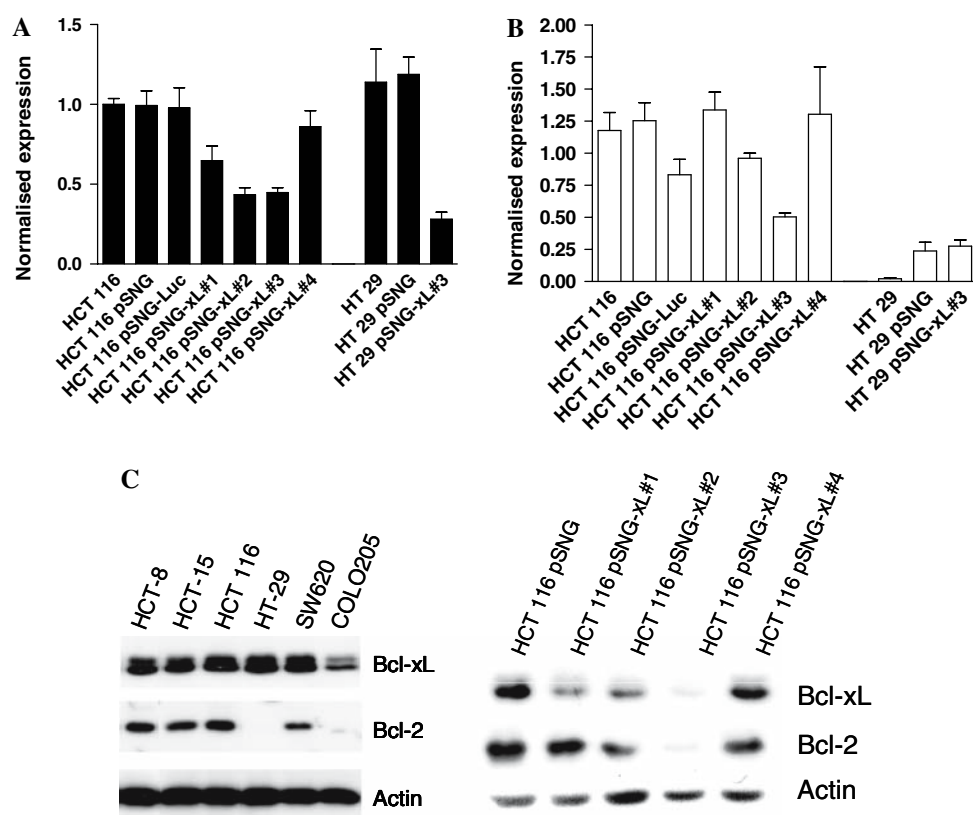


Table 1 Antimycin A3 cytotoxicity in colon cancer cell lines and HCT 116 isogenic cell lines expressing a shRNA against Bcl-xL

| Cell line | IC ₅₀ (μM) |
|-------------------|-----------------------|
| HCT 116 | 0.70 (0.63–0.78) |
| HT-29 | 0.56 (0.48–0.66) |
| SW620 | 0.47 (0.40–0.56) |
| HCT-8 | 0.37 (0.28–0.47) |
| HCT-15 | 0.62 (0.53–0.70) |
| COLO205 | 0.44 (0.39–0.50) |
| HCT 116 pSNG | 0.53 (0.45–0.64) |
| HCT 116 pSNG-Luc | 0.78 (0.72–0.85) |
| HCT 116 pSNG-xL#1 | 0.55 (0.48–0.64) |
| HCT 116 pSNG-xL#1 | 0.41 (0.35–0.49) |
| HCT 116 pSNG-xL#1 | 0.23 (0.2–0.27) |

Cells were exposed to increasing concentrations of Antimycin A3 for 24 h. The growth inhibition was determined by a SRB assay. Results are expressed as mean (95% confidence intervals) of 3–4 experiments performed in triplicate

tive with an $IC_{50} = 0.23 \mu\text{M}$ compared to HCT 116 pSNG ($0.53 \mu\text{M}$). A decrease in Bcl-xL and Bcl-2 expression therefore seems to sensitise cells to AA3.

HCT 116 pSNG-xL cells are more sensitive to topoisomerase I inhibitors

To evaluate the effect of the decrease of Bcl-xL expression (via siRNA expression) on drug sensitivity, we

determined the growth inhibitory effect of topoisomerase I inhibitors SN-38 and camptothecin (CPT) and topoisomerase II inhibitor doxorubicin in the different isogenic cell lines (Table 2). A significant increase in sensitivity was observed with SN-38 in HCT 116 pSNG-xL#2 and 3 ($IC_{50} = 2.1$ and 1.8 nM , respectively) compared to the parental cell line ($IC_{50} = 3.9 \text{ nM}$) or the control siRNA cell line ($IC_{50} = 4.1 \text{ nM}$). A similar effect was observed with camptothecin although the increase in sensitivity was maximal in HCT 116 pSNG-xL#3 cells. However, there was no gain in growth inhibition when exposing the different cell lines to doxorubicin, a topoisomerase II inhibitor: the IC_{50} s ranged from 23.5 nM in HCT 116 to 27.2 nM in HCT 116 pSNG.

SN-38 and AA3 combination recapitulate siRNA effect in HCT 116 cells

The sensitivity to AA3 was related to both Bcl-xL and Bcl-2 expression in HCT 116 pSNG-xL cells. In order to mimic the effect of the siRNA with a small molecule inhibitor, we exposed HCT 116 cells to a sequential combination of SN-38 and AA3 (Fig. 2). The growth inhibitory effect of the combination was greater than both drugs used individually: 50% growth inhibition was induced by combining $0.13 \mu\text{M}$ AA3 with 1.3 nM SN-38 as compared to $0.53 \mu\text{M}$ AA3 and 3.9 nM SN-38

Table 2 SN-38, CPT and Doxorubicin cytotoxicity in HCT 116 isogenic cell lines expressing siRNA against Bcl-xL

| | SN-38 (nM) | CPT (nM) | Dox (nM) |
|-------------------|---------------|---------------|--------------|
| HCT 116 | 3.9 (3.6–4.2) | 8.3 (7.7–8.9) | 23.5 (20–27) |
| HCT 116 pSNG | 3.2 (2.8–3.5) | 8.3 (7.5–9) | 27.2 (22–33) |
| HCT 116 pSNG-Luc | 4.1 (3.7–4.6) | 7.8 (7.3–8.2) | 25.9 (21–30) |
| HCT 116 pSNG-xL#1 | 2.7 (2.5–2.9) | 7.1 (6.6–7.7) | 22.2 (19–26) |
| HCT 116 pSNG-xL#2 | 2.1 (1.9–2.4) | 6.8 (6.5–7.1) | 24.8 (23–26) |
| HCT 116 pSNG-xL#3 | 1.8 (1.3–2.6) | 5.2 (4.6–5.9) | 23.9 (20–27) |

Cells were exposed to increasing concentrations of Antimycin A3 for 24 h. The growth inhibition was determined by a SRB assay. Results are expressed as mean (95% confidence intervals) of 3–4 experiments performed in triplicate

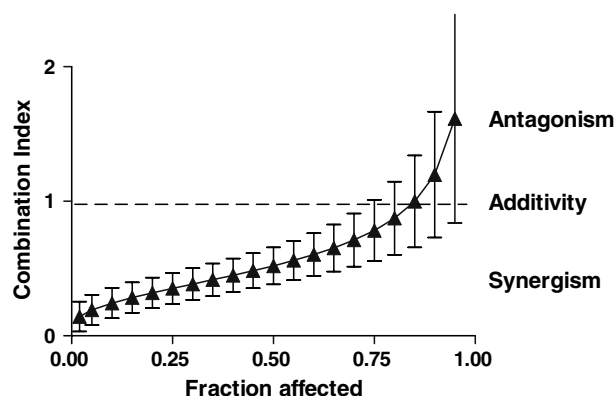


Fig. 2 Median effect plot of the growth inhibitory effect of Antimycin A3 and SN-38 combination in HCT 116 cell line. Cells were exposed to increasing concentrations of Antimycin A3, SN-38 or a combination of both for 24 h at a constant ratio of 100:1. The growth inhibition was determined by a SRB assay 72 h after the end of drug exposure. Results are expressed as mean \pm SD of triplicate samples

when used as single agent. The median effect analysis confirmed the synergistic effect of the combination with a combination index (CI) lower than one.

SN-38 induces differential senescence in HCT 116 pSNG-xL cells

Previous studies have shown that SN-38 can induce both senescence and apoptosis in vitro [11, 27]. The different isogenic cell lines HCT 116 pSNG-xL were exposed to SN-38 for 24 h and the presence of senescent cells was determined 8 days after the end of drug exposure (Fig. 3a). The percentage of senescent cells in the different cell lines varied between 0.05% in HCT 116 pSNG and 0.14% in HCT 116 pSNG-xL#3. At a low concentration (0.5 nM) inducing 0–8% growth inhibition, no significant difference in the percentage of senescent cells was detected among the cell lines (0.6–0.18%). However, at higher concentrations (1 and

2.5 nM) inducing 2–20% and 21–55% of growth inhibition in the various cell lines, HCT 116 pSNG-xL#3 showed the highest increase in SA- β gal positive cells (86-fold at 2.5 nM SN-38). In HCT 116 pSNG-xL#2, despite a similar level of Bcl-xL, SN-38 increased senescent cells by only 36-fold, close to the level observed in HCT 116 pSNG-xL#1. These results were confirmed using PKH2 labelling. The lipophilic fluorophore PKH2 stably incorporates into the plasma membrane and distributes evenly between daughter cells, resulting in gradual decrease in PKH2 fluorescence during successive cell divisions. Cells showing a drug-induced senescence-like phenotype present a high PKH2 content due to growth arrest associated with a DNA content $>4N$ [4]. The DNA analysis of the PKH2^{high} fraction in HCT 116 pSNG-xL cells after exposure to 5 nM SN-38 (Fig. 3b, c) showed that HCT 116 pSNG-xL#2 cells present a lower fraction of cells with a DNA content $>4N$ ($7.7 \pm 1.8\%$) compared to the other isogenic cell lines (14.7 ± 2.9 and 14.6 ± 1.6 for HCT 116 pSNG-xL#1 and 3, respectively).

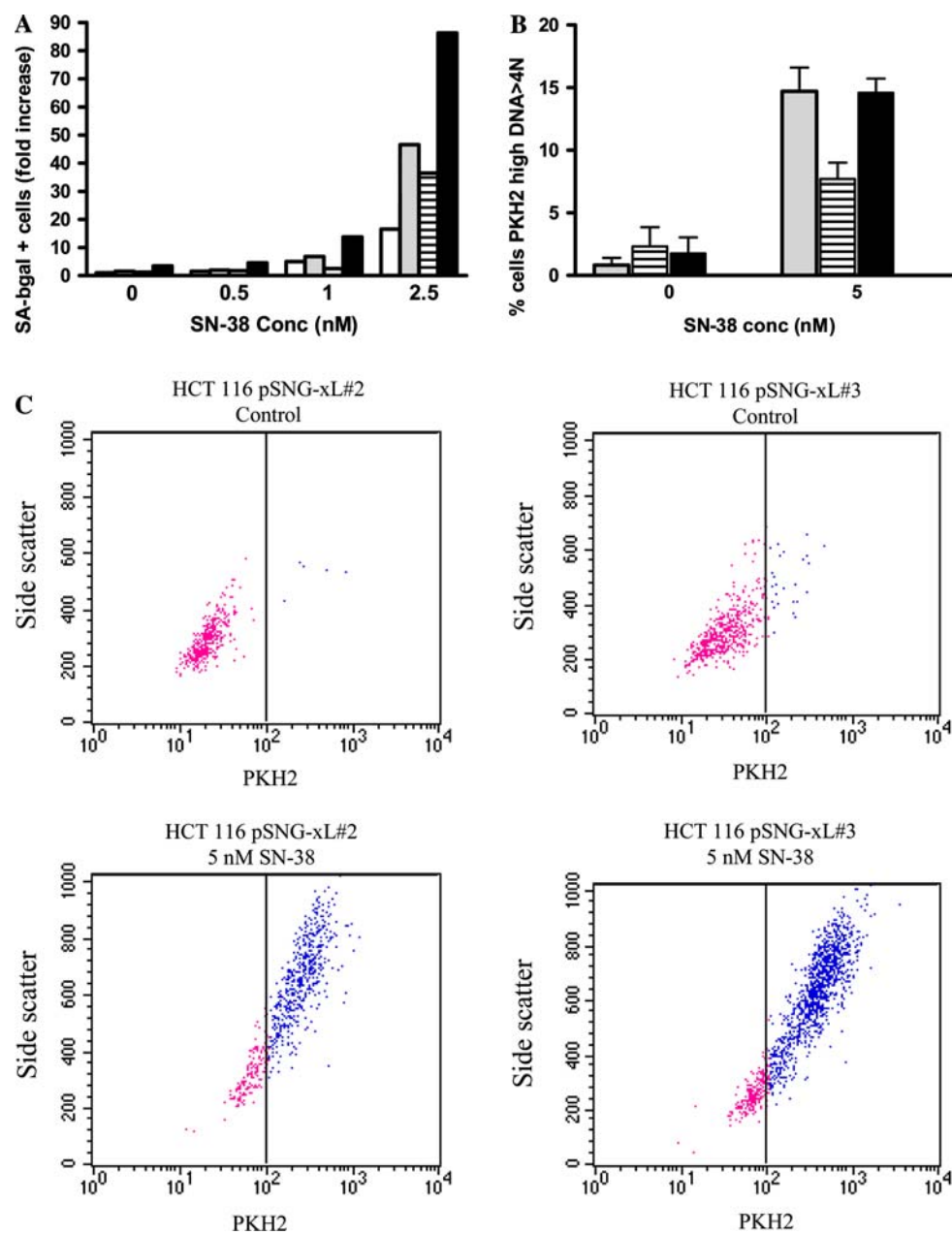
SN-38 induces differential apoptosis in HCT 116 pSNG-xL cells

Loss of mitochondrial membrane potential ($\Delta\Psi_m$) is one of the main events during the apoptotic process. As Bcl-xL blocks the mitochondrial membrane permeabilization and $\Delta\Psi_m$ [14], we evaluated $\Delta\Psi_m$ in the different isogenic cell lines after exposure to SN-38 or CPT using a mitochondrial specific dye JC-1. $\Delta\Psi_m$ was determined by the decrease in JC-1 red fluorescence (FL2 channel). Exposure of HCT 116 pSNG-xL#2 to SN-38 induces a dose-dependent decrease in Ψ_m (FL2 decrease = -33 and -52 , at 5 and 10 nM SN-38, respectively). A similar loss of Ψ_m was observed in HCT 116 pSNG-xL#3 at 5 and 10 nM SN-38 (-39 and -38 , respectively). HCT 116 pSNG-xL#2 also showed a greater decrease in JC-1 fluorescence after 10 or 100 nM CPT than HCT 116 pSNG-xL#3 suggesting that a greater fraction of the cells undergo apoptosis in this cell line.

HCT 116 pSNG-xL#3 xenografts are more sensitive to irinotecan in vivo than HCT 116 pSNG xenografts

As the gain in sensitivity in vitro was maximal for HCT 116 pSNG-xL#3 and SN-38, HCT 116 pSNG and HCT 116 pSNG-xL#3 cell lines were established as xenografts in immunodeficient animals and treated with irinotecan (pro-drug of SN-38) at a dose of 5 mg/kg for five consecutive days. Efficacy was assessed using the time for each xenograft to reach five times its initial volume (T_{5V_0}). T_{5V_0} was not significantly different between HCT 116-

Fig. 3 SN-38 induced senescence. **a** HCT 116 pSNG (Open box), HCT 116 pSNG-xL#1 (Shaded box), HCT 116 pSNG-xL#2 (Striped box), HCT 116 pSNG-xL#3 (Filled box) were exposed to SN-38 for 24 h (0.5–2.5 nM). Cells were stained for SA- β galactosidase detection on day 8 after drug exposure. **b** Determination of the percentage of senescent cells after PKH2 staining: Cells were labelled with PKH2 and exposed to 5 nM SN-38. On day 8, the fraction of cells with high PKH2 content (>100) and DNA content $>4N$ was determined by flow cytometry. Ten thousand events were collected for each analysis. **c** Representative plot of PKH2 fluorescence versus side scatter for HCT 116 pSNG-xL#2 and HCT 116 pSNG-xL#3 cells untreated or exposed to 5 nM SN-38. Cells were analysed on day 8



pSNG and HCT 116 pSNG-xL#3 in untreated animals (Fig. 4a). Irinotecan demonstrated significant anti-tumour activity against both xenografts but the decrease in growth rate and therefore the $T5V_0$ was significantly greater in the HCT 116 pSNG-xL#3: $T5V_0 = 25.5$ days for HCT 116 pSNG-xL#3 xenografts compared to 20.5 days in HCT 116 pSNG. Moreover, 2 HCT 116 pSNG-xL#3 tumours presented complete response (Fig. 5).

Irinotecan induces increased senescence in HCT 116 pSNG-xL#3 xenografts

During the week of treatment with irinotecan, a decrease in growth rate was observed in 7/10 HCT 116

pSNG-xL#3 xenografts but in none (0/10) of the HCT 116 pSNG xenografts. Drug-induced senescence and apoptosis were therefore investigated during this period and four tumour xenografts were examined on days 3, 5 and 7 after irinotecan treatment. No SA- β gal positive cells were detectable on days 3 and 5. On day 7, following treatment of HCT 116 pSNG xenografts with irinotecan, there was no significant increase in the number of senescent cells. In contrast, in the HCT 116 pSNG-xL#3 xenografts, 2/3 xenografts treated with irinotecan contained a greater number of senescent cells than untreated controls. No apoptotic cells could be detected at any time-point in any of the xenografts tested.

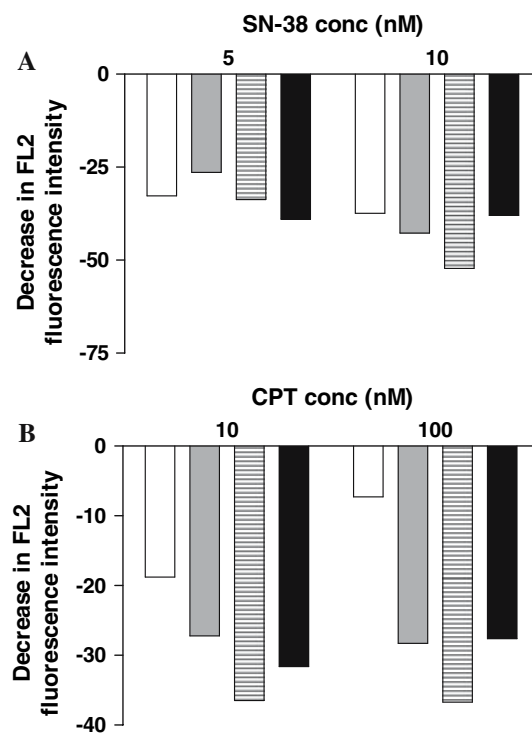


Fig. 4 Loss of mitochondrial membrane potential was determined by the decrease in JC-1 red fluorescence (FL2). HCT 116 pSNG (Open box), HCT 116 pSNG-xL#1 (Shaded box), HCT 116 pSNG-xL#2 (Striped box), HCT 116 pSNG-xL#3 (Filled box) were exposed to SN-38 (a) or CPT (b) for 24 h. JC-1 staining was performed 48 h after drug exposure. Results are expressed as the difference in JC-1 red fluorescence in untreated and treated cells

Discussion

Bcl-xL and Bcl-2 play different roles in cell death and predominance of either protein may influence the cell death mechanism in tumour cells [14]. These effects differ in different cell types and previous studies have highlighted the different phenotypes obtained after overexpression of Bcl-2 or Bcl-xL: resistance to apoptosis [17], premature senescence [8] or even autophagic cell death [22].

In this study, we used a siRNA approach to evaluate the effect of Bcl-xL downregulation in the sensitivity to topoisomerase I inhibitor in colorectal cancer cell lines. Four short hairpin RNA targeting Bcl-xL were expressed in HCT 116 cells. The expression for Bcl-xL and Bcl-2 varied with the siRNA expressed: HCT 116 pSNG-xL#1 and #4 showed a modest (~30%) decrease in Bcl-xL expression whilst Bcl-2 levels were similar to the parental cell line, HCT 116 pSNG-xL#2 showed a 50% decrease in Bcl-xL and no change in Bcl-2 levels. Finally, HCT 116 pSNG-xL#3 showed a concomitant decrease in Bcl-xL and Bcl-2 levels. This is unlikely to

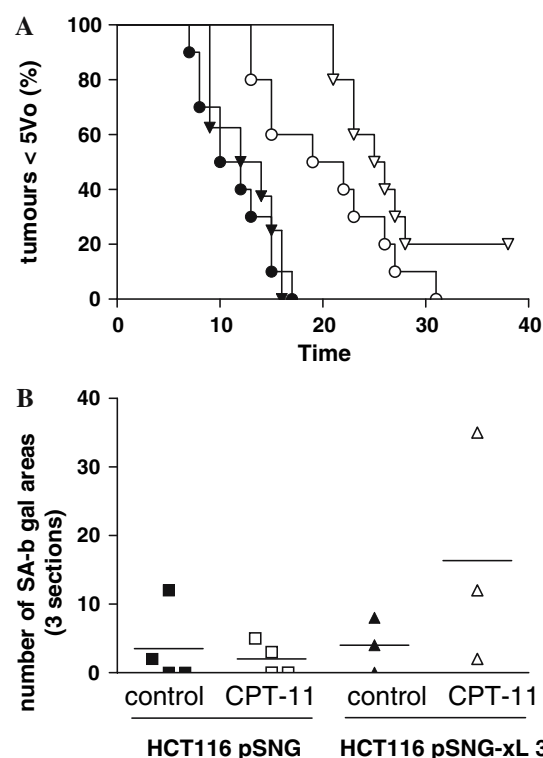


Fig. 5 **a** Irinotecan antitumor activity against HCT 116 pSNG (Filled circle, Open circle) and HCT 116 pSNG-xL#3 (Filled triangle, Open triangle) xenografts. Cells (10^7) were implanted subcutaneously and animals treated on day 7 with vehicle (solid line, closed symbols) or 5 mg/kg irinotecan daily \times 5 (dashed line, open symbols). The tumour growth rate was expressed as the time necessary for each xenograft to reach five times its initial volume. **b** HCT 116 pSNG (square) and HCT 116 pSNG-xL#3 (triangle) xenografts were collected on day 5 of vehicle (closed symbols) or irinotecan treatment (open symbols). Cryosections (three per xenograft) from 3–4 xenografts were stained for SA- β -gal detection and the number of positive areas determined

be due to the cross-reactivity of the siRNA with Bcl-2 sequence since the same construct expressed in HT29 cells did not modify Bcl-2 expression. As the cells expressing the shRNA were selected by geneticin, it is possible that in HCT 116, high levels of Bcl-2 were not sustainable in presence of low levels of Bcl-xL. This would be supported by the data in HT29 in which the low levels of Bcl-2 allowed for a greater downregulation of Bcl-xL. This regulation of expression between Bcl-2 and Bcl-xL has previously been reported by Arriola et al. [1] in testicular cancer in which increase in Bcl-2 levels led to a decrease in Bcl-xL and increased sensitivity to chemotherapy.

To confirm the phenotype of the four isogenic HCT 116 cell lines generated, we evaluated their sensitivity to Antimycin A3, an inhibitor of both Bcl-xL and Bcl-2. Previous studies by Hockenberry et al. showed that AA3 interacts with the Bcl-2 homology domain 3 (BH3)-binding hydrophobic groove of Bcl-xL and

inhibits the pore-forming activity of Bcl-xL in synthetic liposomes [15, 29]. However, contradictory results were obtained: in FL5.12 murine pro-B cells, overexpression of Bcl-xL prevented cell death after exposure to AA3 [30] while in murine hepatocytes, Tzung et al. found sensitisation [29], potentially due to different cellular contexts, as recently pointed out by Letai [16]. In our model system, a decrease in Bcl-xL and/or Bcl-2 sensitised cells to Antimycin A3. However, Antimycin A3 had a similar cytotoxic effect across a panel of colon cancer cell lines with similar Bcl-xL expression but differing in their Bcl-2 expression, suggesting that AA3-induced cell death is related to Bcl-xL rather than Bcl-2 expression, in these cell lines. HA14-1, which displaced BAK-BH3 peptide binding to BCL-2 at high concentrations, showed similar cytotoxicity across the different HCT 116 pSNG-xL lines (data not shown).

A previous study at our laboratory showed that a decrease in Bcl-xL expression using Bcl-xL antisense, sensitised cells to the topoisomerase I inhibitor, SN-38 [11]. Similarly, a decrease in Bcl-xL expression using siRNA increased 5FU sensitivity in 5FU-resistant DLD1 cells [35]. Here we confirm that downregulation of Bcl-xL and/or Bcl-2 sensitised cells to topoisomerase I inhibitors SN-38 and camptothecin but not to doxorubicin. Antimycin A3, in combination with SN-38 recapitulated the phenotype observed in HCT 116 pSNG-xL cells, confirming the role of Bcl-xL in this synergy.

The four cell lines generated displayed different Bcl-xL/Bcl-2 ratios and were used to shed light on the mechanisms of cell death related to the gain in sensitivity to SN-38. SN-38 was previously shown to induce a SLP in HCT 116 [27], but apoptosis has also been reported in a number of other model systems [19, 25, 26].

Exposure of HCT 116 pSNG-xL#1 to SN-38 was associated with a moderate increase in both senescence and loss of mitochondrial membrane potential ($\Delta\Psi_m$) and a modest increase in SN-38 induced global cytotoxicity. A greater decrease in Bcl-xL expression whilst the levels of Bcl-2 were maintained, (HCT 116 pSNG-xL#2) led to an increase in apoptosis (loss of $\Delta\Psi_m$) and reduced senescence after SN-38 exposure. These changes were associated with a greater growth inhibitory effect of SN-38. Finally, when both Bcl-xL and Bcl-2 were decreased to a similar degree (HCT 116 pSNG-xL#3), senescence was significantly increased but loss of $\Delta\Psi_m$ was limited. A specific decrease in Bcl-xL therefore led to increased apoptosis. Bcl-xL but not Bcl-2 inhibits DISC formation in the extrinsic pathway. In HCT 116 pSNG-xL#2, the specific decrease in Bcl-xL expression could therefore potentiate SN-38 cytotoxic effect by increasing DR4 and DR5-mediated

cell death. Irinotecan and TRAIL exert a synergistic cytotoxic effect in HCT 116 cells due to a greater induction of DR4 and DR5 expression and inhibition of DcR1, DcR2 induction observed after irinotecan alone [34].

The concomitant decrease in Bcl-xL and Bcl-2 in HCT 116 pSNG-xL#3 induced greater SLP than apoptosis after SN-38 exposure. Although SLP has been postulated to occur at low drug concentrations, maximum senescence was observed in HCT 116 cells after 200 nM doxorubicin (ten times the IC_{50}) [6] and was observed with different chemotherapeutic agents at concentrations inhibiting 85% of cell growth [4]. The concentrations of SN-38 used in this study are therefore consistent with these previous reports. Similarly, the number of senescent cells increased 16–80 times after exposure to SN-38 in HCT 116 pSNG-xL cell lines and was correlated with Bcl-xL expression. This is consistent with the up to 60-fold increase in doxorubicin-induced SLP in HCT 116 cells [5]. The timing used to determine senescence and apoptosis (loss of $\Delta\Psi_m$) was important: SA- β galactosidase staining was carried out on day 8 and loss of $\Delta\Psi_m$ on day 4 while the growth inhibitory effect of SN-38 was determined on day 6. Therefore, it is likely that a fraction of the surviving cells determined on day 6 by SRB were in fact senescent. In HCT 116 pSNG-xL#3, PKH2 labelling previously described by Chang et al. [4], confirmed that the overall growth inhibitory effect induced by SN-38 was mainly due to growth arrest evolving into senescence. This effect was confirmed *in vivo* after administration of irinotecan, a prodrug of SN-38, and was associated with greater antitumour effect.

In summary, our studies demonstrate that a decrease in Bcl-xL expression leads to a sensitisation to topoisomerase I inhibitor SN-38. The relative expression of Bcl-xL and Bcl-2 although leading to similar growth inhibitory effect with SN-38, controls drug-induced senescence and apoptosis. Optimal growth inhibitory effect was observed when both Bcl-xL and Bcl-2 were decreased to a similar extent. The same effect was achievable using the small molecule, antimycin A3, adding further support to the development of small molecule inhibitors of the Bcl-xL/Bcl-2 family and their testing in the treatment of colorectal cancer.

Acknowledgments We are very grateful to Prof. Hockenberry for providing Antimycin A3.

References

1. Arriola EL, Rodriguez-Lopez AM, Hickman JA, Chresta CM (1999) Bcl-2 overexpression results in reciprocal

downregulation of Bcl-X(L) and sensitizes human testicular germ cell tumours to chemotherapy-induced apoptosis. *Oncogene* 18:1457

2. Backus HH, Van Groeningen CJ, Vos W, Dukers DF, Bloemena E, Wouters D, Pinedo HM, Peters GJ (2002) Differential expression of cell cycle and apoptosis related proteins in colorectal mucosa, primary colon tumours, and liver metastases. *J Clin Pathol* 55:206
3. Bertrand JR, Pottier M, Vekris A, Opolon P, Maksimenko A, Malvy C (2002) Comparison of antisense oligonucleotides and siRNAs in cell culture and in vivo. *Biochem Biophys Res Commun* 296:1000
4. Chang BD, Broude EV, Dokmanovic M, Zhu H, Ruth A, Xuan Y, Kandel ES, Lausch E, Christov K, Roninson IB (1999) A senescence-like phenotype distinguishes tumor cells that undergo terminal proliferation arrest after exposure to anticancer agents. *Cancer Res* 59:3761
5. Chang BD, Xuan Y, Broude EV, Zhu H, Schott B, Fang J, Roninson IB (1999) Role of p53 and p21waf1/cip1 in senescence-like terminal proliferation arrest induced in human tumor cells by chemotherapeutic drugs. *Oncogene* 18:4808
6. Chang BD, Swift ME, Shen M, Fang J, Broude EV, Roninson IB (2002) Molecular determinants of terminal growth arrest induced in tumor cells by a chemotherapeutic agent. *Proc Natl Acad Sci USA* 99:389
7. Chou TC, Talalay P (1984) Quantitative analysis of dose-effect relationships: the combined effects of multiple drugs or enzyme inhibitors. *Adv Enzyme Regul* 22:27
8. Crescenzi E, Palumbo G, Brady HJ (2003) Bcl-2 activates a programme of premature senescence in human carcinoma cells. *Biochem J* 375:263
9. Dallas A, Vlassov AV (2006) RNAi: A novel antisense technology and its therapeutic potential. *Med Sci Monit* 12:RA67
10. Elbashir SM, Harborth J, Lendeckel W, Yalcin A, Weber K, Tuschl T (2001) Duplexes of 21-nucleotide RNAs mediate RNA interference in cultured mammalian cells. *Nature* 411:494
11. Hayward RL, Macpherson JS, Cummings J, Monia BP, Smyth JF, Jodrell DI (2003) Antisense Bcl-xL down-regulation switches the response to topoisomerase I inhibition from senescence to apoptosis in colorectal cancer cells, enhancing global cytotoxicity. *Clin Cancer Res* 9:2856
12. Ho HK, Hu ZH, Tzung SP, Hockenberry DM, Fausto N, Nelson SD, Bruschi SA (2005) BCL-xL overexpression effectively protects against tetrafluoroethylcysteine-induced intramitochondrial damage and cell death. *Biochem Pharmacol* 69:147
13. Holt SE, Aisner DL, Shay JW, Wright WE (1997) Lack of cell cycle regulation of telomerase activity in human cells. *Proc Natl Acad Sci USA* 94:10687
14. Kim R (2005) Unknotting the roles of Bcl-2 and Bcl-xL in cell death. *Biochem Biophys Res Commun* 333:336
15. Kim KM, Giedt CD, Basanez G, O'Neill JW, Hill JJ, Han YH, Tzung SP, Zimmerberg J, Hockenberry DM, Zhang KY (2001) Biophysical characterization of recombinant human Bcl-2 and its interactions with an inhibitory ligand, antimycin A. *Biochemistry* 40:4911
16. Letai A (2005) Pharmacological manipulation of Bcl-2 family members to control cell death. *J Clin Invest* 115:2648
17. Letai A, Sorcinelli MD, Beard C, Korsmeyer SJ (2004) Antia apoptotic BCL-2 is required for maintenance of a model leukemia. *Cancer Cell* 6:241
18. Maurer CA, Friess H, Buhler SS, Wahl BR, Gruber H, Zimermann A, Buchler MW (1998) Apoptosis inhibiting factor Bcl-xL might be the crucial member of the Bcl-2 gene family in colorectal cancer. *Dig Dis Sci* 43:2641
19. Minderman H, Conroy JM, O'Loughlin KL, McQuaid D, Quinn P, Li S, Pendyala L, Nowak NJ, Baer MR (2005) In vitro and in vivo irinotecan-induced changes in expression profiles of cell cycle and apoptosis-associated genes in acute myeloid leukemia cells. *Mol Cancer Ther* 4:885
20. Schmitt CA, Fridman JS, Yang M, Lee S, Baranov E, Hoffman RM, Lowe SW (2002) A senescence program controlled by p53 and p16INK4a contributes to the outcome of cancer therapy. *Cell* 109:335
21. Shay JW, Roninson IB (2004) Hallmarks of senescence in carcinogenesis and cancer therapy. *Oncogene* 23:2919
22. Shimizu S, Kanaseki T, Mizushima N, Mizuta T, Arakawa-Kobayashi S, Thompson CB, Tsujimoto Y (2004) Role of Bcl-2 family proteins in a non-apoptotic programmed cell death dependent on autophagy genes. *Nat Cell Biol* 6:1221
23. Shoemaker AR, Oleksijew A, Bauch J, Belli BA, Borre T, Bruncko M, Deckwirth T, Frost DJ, Jarvis K, Joseph MK, Marsh K, McClellan W, Nellans H, Ng S, Nimmer P, O'Connor JM, Oltersdorf T, Qing W, Shen W, Stavropoulos J, Tahir SK, Wang B, Warner R, Zhang H, Fesik SW, Rosenberg SH, Elmore SW (2006) A Small-molecule inhibitor of Bcl-XL potentiates the activity of cytotoxic drugs in vitro and in vivo. *Cancer Res* 66:8731
24. Skehan P, Storeng R, Scudiero D, Monks A, McMahon J, Vistica D, Warren JT, Bokesch H, Kenney S, Boyd MR (1990) New colorimetric cytotoxicity assay for anticancer-drug screening. *J Natl Cancer Inst* 82:1107
25. Tanaka R, Ariyama H, Qin B, Shibata Y, Takii Y, Kusaba H, Baba E, Mitsugi K, Harada M, Nakano S (2005) Synergistic interaction between oxaliplatin and SN-38 in human gastric cancer cell lines in vitro. *Oncol Rep* 14:683
26. te Poole RH, Joel SP (1999) Schedule-dependent cytotoxicity of SN-38 in p53 wild-type and mutant colon adenocarcinoma cell lines. *Br J Cancer* 81:1285
27. te Poole RH, Okorokov AL, Jardine L, Cummings J, Joel SP (2002) DNA damage is able to induce senescence in tumor cells in vitro and in vivo. *Cancer Res* 62:1876
28. Tuschl T (2001) RNA interference and small interfering RNAs. *Chembiochem* 2:239
29. Tzung SP, Kim KM, Basanez G, Giedt CD, Simon J, Zimmerberg J, Zhang KY, Hockenberry DM (2001) Antimycin A mimics a cell-death-inducing Bcl-2 homology domain 3. *Nat Cell Biol* 3:183
30. Vander Heiden MG, Chandel NS, Williamson EK, Schumacker PT, Thompson CB (1997) Bcl-xL regulates the membrane potential and volume homeostasis of mitochondria. *Cell* 91:627
31. Vidal L, Blagden S, Attard G, de Bono J (2005) Making sense of antisense. *Eur J Cancer* 41:2812
32. Wang X, Zhang J, Kim HP, Wang Y, Choi AM, Ryter SW (2004) Bcl-XL disrupts death-inducing signal complex formation in plasma membrane induced by hypoxia/reoxygenation. *Faseb J* 18:1826
33. Williams J, Lucas PC, Griffith KA, Choi M, Fogoros S, Hu YY, Liu JR (2005) Expression of Bcl-xL in ovarian carcinoma is associated with chemoresistance and recurrent disease. *Gynecol Oncol* 96:287
34. Xiang H, Fox JA, Totpal K, Aikawa M, Dupree K, Sinicrope D, Lowe J, Escandon E (2002) Enhanced tumor killing by Apo2L/TRAIL and CPT-11 co-treatment is associated with p21 cleavage and differential regulation of Apo2L/TRAIL ligand and its receptors. *Oncogene* 21:3611
35. Zhu H, Guo W, Zhang L, Davis JJ, Teraishi F, Wu S, Cao X, Daniel J, Smythe WR, Fang B (2005) Bcl-XL small interfering RNA suppresses the proliferation of 5-fluorouracil-resistant human colon cancer cells. *Mol Cancer Ther* 4:451